HHS Public Access

Author manuscript

*J Am Chem Soc*. Author manuscript; available in PMC 2019 July 16.

Published in final edited form as:

*J Am Chem Soc*. 2019 January 16; 141(2): 769–773. doi:10.1021/jacs.8b12010.

# Genome-mined Diels-Alderase catalyzes formation of the *cis*-octahydrodecalins of varicidin A and B

**Dan Tan**[#1,2], **Cooper S. Jamieson**[#3], **Masao Ohashi**[2], **Man-Cheng Tang**[2], **K. N. Houk**[3], and **Yi Tang**[2,3]

[1]Key Laboratory of Biomedical Information Engineering of Ministry of Education, School of Life Science and Technology, Xi'an Jiaotong University, Xi'an, 710049, P. R. China

[2]Departments of Chemical and Biomolecular Engineering, University of California, Los Angeles, California 90095, United States.

[3]Chemistry and Biochemistry, University of California, Los Angeles, California 90095, United States.

[#] These authors contributed equally to this work.

## Abstract

Pericyclases are an emerging family of enzymes catalyzing pericyclic reactions. A class of lipocalin-like enzymes recently characterized as Diels-Alderases (DAses) catalyze decalin formation through intramolecular Diels-Alder (IMDA) reactions between electron-rich dienes and electron-deficient dienophiles. Using this class of enzyme as a beacon for genome mining, we discovered a biosynthetic gene cluster from *Penicillium variabile* and identified that it encodes for the biosynthesis of varicidin A (**1**), a new antifungal natural product containing a *cis*-octahydrodecalin core. Biochemical analysis reveals a carboxylative deactivation strategy used in varicidin biosynthesis to suppress the nonenzymatic IMDA reaction of an early acyclic intermediate that favors *trans*-decalin formation. A P450 oxidizes the reactive intermediate to yield a relatively unreactive combination of an electron-deficient diene and an electron-deficient dienophile. The DAse PvhB catalyzes the final stage IMDA on the carboxylated intermediate to form the *cis*-decalin that is important for the antifungal activity.

## Graphical Abstract

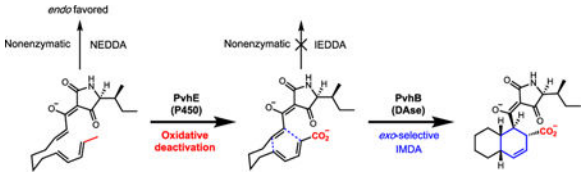


Corresponding Authors yitang@ucla.edu, houk@chem.ucla.edu, tmc19@163.com.

ASSOCIATED CONTENT

Supporting Information

Experimental details, spectroscopic and computational data are available free of charge via the Internet at http://pubs.acs.org.

Pericyclic reactions such as cycloadditions are often used by synthetic chemists to synthesize complex natural products (NPs). One of the most ubiquitous pericyclic reactions is the Diels-Alder (DA) reaction between a 1,3-diene and a dienophile (alkene) to form an unsaturated six-membered ring with up to four stereocenters in a regioselective and stereoselective manner.[1–3] Both normal- and inverse-electron demand DA reactions (NEDDA and IEDDA, respectively) are known, with the former being more common in synthetic chemistry.[4–6] These reactions differ in the frontier molecular orbital (HOMO and LUMO) energy levels of the dienes and dienophiles involved in the reactions.[7–9] Thousands of NPs have been identified to contain fused carbocycles or heterocycles, which led to identification of pericyclases: enzymes that catalyze pericyclic reactions.[10] The most prevalent pericyclases are Diels-Alderases (DAses), such as SpnF, PyrE3, Pyrl4 and AbyU.[11–15] One emerging class of fungal DAses have sequence homology to lipocalin-like enzymes, which bind to steroids and other hydrophobic molecules.[16, 17] They are usually encoded in biosynthetic gene clusters containing a polyketide synthase-nonribosomal peptide synthetase (PKS-NRPS), and perform an intramolecular DA (IMDA) reaction on the immediate product of the PKS-NRPS.[18–20] To date, reactions catalyzed by this family of enzymes, such as CghA[17], MycB[21] and Fsa2[22], are all NEDDA and proceed via the *endo* transition state to yield *trans*-decalin products with different facial stereoselectivities (Figure 1).

Combinatorial pairing of PKS-NRPS and DAses from different biosynthetic gene clusters has led to new decalin compounds, demonstrating the potential of these enzymes in diversification of NPs structures. [23, 24] A large number of cryptic biosynthetic gene clusters can be found in sequenced fungal genomes using the lipocalin DAse such as MycB[21] as the search query. We therefore reasoned that DAses with distinct functions to generate different core structures may be found among these gene clusters. In this work, we focused on a compact gene cluster found in *Penicillium variabile* that encodes a DAse sharing low sequence homology with the characterized ones (36% and 27% sequence identities to Fsa2 and MycB, respectively, Figure S1). The *pvh* cluster also encodes a PKS-NRPS (*pvhA*), a *trans*-acting enoylreductase (ER) (*pvhC*), a putative DAse (*pvhB*), a predicted *N*-methyltransferase (*pvhD*), and a cytochrome P450 (*pvhE*) (Figure 1B and Table S1). No known decalin-containing NPs have been isolated from *P. variabile*.

The five genes (*pvhA-E*) were introduced into an engineered *Aspergillus nidulans* expression host[17] on three episomal vectors (Figure S10 and Table S2, S3). Compared to the negative control, the extract contained a new metabolite **1** with molecular weight (MW) of 375 (Figure 2A, trace i). This compound was isolated and characterized by 1D- and 2D-NMR spectroscopy to be a tetramate-containing decalin (Figures S15-S20, Tables S5). Based on NOESY, the decalin ring of **1** (named varicidin A) is in the *cis* configuration and is carboxylated at C21 (Figure 2B). The amide nitrogen in the 2,4-pyrrolidinedione ring is methylated and is consistent with the coexpression of a *N*-methyltransferase PvhD. Expression of *pvh* gene cluster without *pvhD* in *A. nidulans* led to the biosynthesis of a new compound **2** (varicidin B), which was shown by NMR to be the *N*-desmethyl variant of **1** (Figure 2A, trace ii, Figure S21-S26 and Table S6). We were able to obtain an X-ray crystal structure of **2** (Figure 2D), which allowed us to confirm the *S*-stereochemistry at C17 and

the absolute stereochemistry of **2**. The absolute stereochemistry of **1** was assigned based on that of **2** (Figure 2B). The structure and stereochemistry of the C17 branched chain indicate the incorporation of L-isoleucine by the NRPS module. Both **1** and **2** exhibited antifungal activities against *Candida albicans*[25] with minimum inhibitory concentrations (MICs) of 8 and 16 μg/mL, respectively (Figure S11).

Presumably, the *cis*-decalin structures of **1** and **2** would be formed by *exo*-IMDA reactions from acyclic precursors, and PvhB represents the most likely enzyme to catalyze this diastereoselective reaction, as no isomeric cycloadducts can be detected in the extracts. To confirm the function of PvhB, we only expressed the PKS-NRPS PvhA and its partnering ER PvhC in *A. nidulans*. Analysis of the extract showed the accumulation of **3–5** with the same MW of 331. **3** is an acyclic tetramate (Figure S27-S31 and Table S7). Based on previous studies on decalin-containing NPs such as equisetin[22] and Sch210972[17], the biosynthesis of **3** is expected to follow the similar logic: the PKS domains iteratively synthesize the polyketide portion. Selective enoylreduction by the ER during different cycles furnishes both the diene and the dienophile. The polyketide acyl chain is then condensed with L-isoleucine, followed by a Dieckmann cyclization to afford **3**.[17, 21–22] Compounds **4** and **5** were purified by chiral HPLC and structurally elucidated to be *trans*-decalin diastereomers (Figure S32-S43 and Table S8-S9), which are expected to be derived from the *endo*-specific IMDA reactions from **3**.[17, 21–22] When **3** was left in buffer at pH 7.0, nonenzymatic formation of **4** and **5** can be observed (Figure S2A), consistent with the heterologous expression results in Figure 2A in which **4** and **5** were co-isolated. A mixture of other products was also detected, but the yields were too low for structural characterization (Figure S2C). In agreement with experimental data which showed the rate constant ($k_{non}$) of the nonenzymatic IMDA reaction of **3** was ~ $4.0\times10^{-4}$ $min^{-1}$ in HEPES buffer at 30°C (Figure S3), the density functional theory (DFT) calculations[26–28] at the M06–2X/6–311+G(d,p)/CPCM($H_2O$)//M06–2X/6–31G(d)/SMD($H_2O$) level of theory predicted this value $k_{non,\ calc}$ to be $1.1\times10^{-5}$ $min^{-1}$ (Figure 3A, Figure S12, **TS-1** $\Delta G^{\ddagger}$=26.6 kcal·$mol^{-1}$ and **TS-2** $\Delta G^{\ddagger}$=26.8 kcal·$mol^{-1}$ for **4** and **5**, respectively). In **TS-1** and **TS-2**, secondary orbital interactions of the diene and tetramate carbonyl favor these *endo*-cyclizations. DFT predicts the product mixture contains one *exo*-cycloadduct in similar yield (Figure S12).

Coexpressing PvhAC with PvhB did not change the metabolite profile, with **3–5** remained as the main products (Figure 2A, iv), indicating **3** is not a substrate of PvhB. PvhB was expressed and purified from *E. coli* following codon optimization (Figure S9, Table S4). Adding PvhB to **3** further confirmed that no *cis*-decalin products can be formed (Figure S2A). To determine the timing and substrate of PvhB, we coexpressed PvhAC together with P450 PvhE in *A. nidulans*, which produced a new metabolite **6** (Figure 2A, trace v). NMR analysis showed it to be the carboxylated version of **3** (Figure S44-S48 and Table S10). PvhE was then expressed in *Saccharomyces cerevisiae* RC01,[29] and whole-cell biotransformation was performed by feeding 5 mM of either **3** or a mixture of **4** and **5**. Whereas the acyclic **3** was oxidized to **6** readily, neither the *trans*-decalin compounds were modified (Figure S4). This confirms the role of PvhE in catalyzing oxidation of the C21 methyl group in **3** to the carboxylate in **6**. An additional heterologous expression construct

was made by coexpressing the *N*-methyltransferase PvhD with PvhACE, yielding a new compound **7** (Figure 2, trace vi), which was structurally determined to be the *N*-methylated version of **6** (Figure S49-S53 and Table S11). Recombinant PvhD purified from *E. coli* (Figure S9) was able to completely methylate **6** to **7** in the presence of *S*-adenosylmethionine (SAM), while unable to methylate **2** into **1** (Figure S5). Therefore, the function and timing of PvhD were confirmed to act on **6** to give **7** (Figure 2B).

Notably, replacing the electron-donating methyl in **3** by the electron-withdrawing carboxylate in **6** (and **7**) significantly suppressed nonenzymatic IMDA reactions. Incubation of **6** and **7** in various solvents, even at high temperatures, did not lead to formation of any IMDA products (Figure S6). In solution near neutral pH, oxidized **6** and **7** are expected to exist as dianions.[30] Consequential electrostatic repulsion between the two anions increases the reaction barrier, suppressing the nonenzymatic IMDA reaction. The poor reactivity can also be explained by the pairing of an electron-deficient diene and an electron-deficient dienophile. The dienylcarboxylate and the alkylidenetetramate withdraw electron-density from the diene and dienophile, respectively, increasing the reaction barrier. Furthermore, oxidation alters the electronic nature of the IMDA, switching the reaction type from NEDDA to IEDDA (Figure S13). We believe that both the electrostatic anion repulsion and the electron-deficient nature of diene and dienophile raise the barrier of **7** to the *endo* **TS-3** and the *exo* **TS-4** that leads to **1** to $\Delta G^{\ddagger}$=32.5 and $\Delta G^{\ddagger}$=31.2 kcal·mol$^{-1}$, respectively (Figure 3B). This is a 10,000-fold decrease in rate compared to the nonenzymatic cyclizations of **3**. These IEDDA cycloadditions are predicted to be slow ($k_{non,\ calc}$ = 4.6×10$^{-9}$ min$^{-1}$, Figure 3B) at room temperature, and experimentally no reaction is observed (Figure S6). We hypothesize that protonation may play an important role in catalysis (Figure S14). To investigate the potential modes of catalysis by the enzyme, we explored the possible influence of protonation of the tetramate. Such a protonation is unusual and unlikely in solution as the pKa of the carboxylate is greater than that of the tetramate.[30] We calculated that *exo* reaction of the dienylcarboxylate with the protonated alkylidene tetramic acid lowers the activation energy to form **1** by 3.9 kcal·mol$^{-1}$ via **TS-6** (Figure 3C). Therefore, depending on the protonation state of the tetramic acid in the enzyme active site, these cyclizations could either be NEDDA or IEDDA in presence of PvhB (Figure S13).

These results indicate the DAse PvhB must lower the high barrier of the IEDDA TS in catalyzing the cycloaddition of **6** or **7** to *cis*-decalin **2** or **1**, respectively (Figure 2A). This was verified by *in vitro* assay of purified PvhB, showing that more than 95% of **7** or **6** was converted to **1** or **2** respectively when incubated with PvhB within 12 hrs (Figure 2C, trace iv, ii). Kinetic measurements showed PvhB to have a $K_M$ of 571.6 ± 69.3 μM and $k_{cat}$ of 2.6 ± 0.1 min$^{-1}$ toward **6;** and $K_M$ of 550.1 ± 36.7 μM and $k_{cat}$ of 37.5 ± 3.5 min$^{-1}$ toward **7** (Figure 2B and Figure S7). The 15-fold higher specificity ($k_{cat}/K_M$) of PvhB toward **7** over **6** indicated that **7** is most likely the native substrate of PvhB. This allowed us to propose the overall biosynthetic pathway in which PvhB-catalyzed IMDA reaction is the final step (Figure 2B). We added a strong Lewis acid $SnCl_4$ to **6** in dichloromethane to examine outcomes of the chemical catalysis. However, the Lewis acid gave complex mixtures with compound **2** being a minor product (Figure S8). PvhB is therefore a strong and stereo-

selective DAse to catalyze formation of a single *exo*-specific *cis*-decalin product from the acyclic precursors.

Collectively, we propose a “carboxylative deactivation” strategy used in this biosynthetic pathway to construct the antifungal **1**. Our results show that the activity of redox enzymes can influence the course of biosynthetic pathways that involve IMDA reactions. The acyclic PKS-NRPS product **3** is prone to nonenzymatic IMDA to yield the *trans*-decalin products **4** and **5**. Oxidation of the diene portion of **3** to the dienocarboxylate **6** significantly increases the IMDA barrier and effectively suppresses the nonenzymatic reactions. This can be overcome by the activities of the stereospecific DAse PvhB to arrive at the desired *cis*-decalin product. The discovery of PvhB further illustrates the functional diversity of the lipocalin-like DAses in fungi, and the prospects of using these enzymes as beacons for new natural product discovery.

## Supplementary Material

Refer to Web version on PubMed Central for supplementary material.

## ACKNOWLEDGMENTS

This work was supported by the NIH 1R35GM118056 to YT, NSF (CHE-1806581) to YT and KNH, and NSF of China (21602171) to DT. Chemical characterization studies were supported by shared instrumentation grants from the NSF (CHE-1048804) and the NIH NCRR (S10RR025631). The computational resources from the UCLA Institute of Digital Research and Education (IDRE) are gratefully acknowledged. We thank Yiu Sun Hung for assistance with fungal transformations.

## REFERENCES

1. Nicolaou KC; Snyder SA; Montagnon T; Vassilikogiannakis G The Diels-Alder Reaction in Total Synthesis. Angew. Chem. Int. Ed. Engl 2002 41, 1668–1698. [PubMed: 19750686]
2. Ohashi M; Liu F; Hai Y; Chen M; Tang MC; Yang Z; Sato M; Watanabe K; Houk KN; Tang Y SAM-Dependent Enzyme-Catalysed Pericyclic Reactions in Natural Product Biosynthesis. Nature 2017, 549, 502–506. [PubMed: 28902839]
3. Funel JA; Abele S Industrial Applications of the Diels-Alder Reaction. Angew. Chem. Int. Ed. Engl 2013, 52, 3822–3863. [PubMed: 23447554]
4. Patel PR; Boger DL Intramolecular Diels-Alder Reactions of Cyclopropenone Ketals. Org. Lett 2010, 12, 3540–3543 [PubMed: 20614867]
5. Bodwell G,J; Pi Z Electron deficient dienes I. Normal and Inverse Electron Demand Diels-Alder Reaction of the Same Carbon Skeleton. Tetrahedron Lett 1997, 38, 309–312.
6. Saha S; Roy RK; Pal S CDASE-A Reliable Scheme to Explain the Reactivity Sequence Between Diels-Alder Pairs. Phys. Chem. Chem. Phys 2010, 12, 9328–9338. [PubMed: 20601981]
7. Spino C; Rezaei H; Dory YL Characteristics of the Two Frontier Orbital Interactions in the Diels-Alder Cycloaddition. J. Org. Chem 2004, 69, 757–764. [PubMed: 14750802]
8. Levandowski BJ; Hamlin TA; Bickelhaupt FM; Houk KN Role of Orbital Interactions and Activation Strain (Distortion Energies) on Reactivities in the Normal and Inverse Electron-Demand Cycloadditions of Strained and Unstrained Cycloalkenes. J. Org. Chem 2017, 82, 8668–8675. [PubMed: 28712288]
9. Oliveira BL; Guo Z; Bernardes GJL Inverse Electron Demand Diels-Alder Reactions in Chemical Biology. Chem. Soc. Rev 2017, 46, 4895–4950. [PubMed: 28660957]
10. Jamieson CS; Ohashi M; Liu F; Tang Y; Houk KN The Expanding World of Biosynthetic Pericyclases: Cooperation of Experiment and Theory for Discovery. Nat. Prod. Rep 2018 DOI: 10.1039/c8np00075a.

11. Takao K; Munakata R; Tadano K Recent Advances in Natural Product Synthesis by Using Intramolecular Diels-Alder Reactions. Chem. Rev 2005, 105, 4779–4807. [PubMed: 16351062]
12. Kim HJ; Ruszczycky MW; Choi SH; Liu YN; Liu HW Enzyme-Catalysed [4+2] Cycloaddition Is a Key Step in the Biosynthesis of Spinosyn A. Nature 2011, 473, 109–112. [PubMed: 21544146]
13. Fage CD; Isiorho EA; Liu Y; Wagner DT; Liu HW; Keatinge-Clay AT The Structure of SpnF, a Standalone Enzyme that Catalyzes [4 + 2] Cycloaddition. Nat. Chem. Biol 2015, 11, 256–258. [PubMed: 25730549]
14. Tian Z; Sun P; Yan Y;, Wu Z; Zheng Q; Zhou S; Zhang H; Yu F; Jia X; Chen D; Mándi A; Kurtán T; Liu W An Enzymatic [4+2] Cyclization Cascade Creates the Pentacyclic Core of Pyrroindomycins. Nat. Chem. Biol 2015, 11, 259–265. [PubMed: 25730548]
15. Byrne MJ; Lees NR; Han LC; van der Kamp MW; Mulholland AJ; Stach JE; Willis CL; Race PR The Catalytic Mechanism of a Natural Diels-Alderase Revealed in Molecular Detail. J. Am. Chem. Soc 2016, 138, 6095–6098. [PubMed: 27140661]
16. Flower DR; North AC; Sansom CE The Lipocalin Protein Family: Structural and Sequence Overview. Biochim. Biophys. Acta 2000,1482, 9–24. [PubMed: 11058743]
17. Sato M; Yagishita F; Mino T; Uchiyama N; Patel A; Chooi YH; Goda Y; Xu W; Noguchi H; Yamamoto T; Hotta K; Houk KN; Tang Y; Watanabe K Involvement of Lipocalin-Like CghA in Decalin-Forming Stereoselective Intramolecular [4+2] Cycloaddition. Chem. Bio. Chem 2015, 16, 2294–2298.
18. Qiao K; Chooi YH; Tang Y Identification and Engineering of the Cytochalasin Gene Cluster from Aspergillus clavatus NRRL 1. Metab. Eng 2011, 13, 723–732. [PubMed: 21983160]
19. Oikawa H; Tokiwano T Enzymatic Catalysis of the Diels-Alder Reaction in the Biosynthesis of Natural Products. Nat. Prod. Rep 2004, 21, 321–352. [PubMed: 15162222]
20. Minami A; Oikawa H Recent Advances of Diels-Alderases Involved in Natural Product Biosynthesis. J. Antibiot 2016, 69, 500–506. [PubMed: 27301662]
21. Li L; Yu P; Tang MC; Zou Y; Gao SS; Hung YS; Zhao M; Watanabe K; Houk KN; Tang Y Biochemical Characterization of a Eukaryotic Decalin-Forming Diels-Alderase. J. Am. Chem. Soc 2016, 138, 15837–15840. [PubMed: 27960349]
22. Kato N; Nogawa T; Hirota H; Jang JH; Takahashi S; Ahn JS; Osada H A New Enzyme Involved in the Control of the Stereochemistry in the Decalin Formation during Equisetin Biosynthesis. Biochem. Biophys. Res. Commun 2015, 460, 210–215. [PubMed: 25770422]
23. Kato N; Nogawa T; Takita R; Kinugasa K; Kanai M; Uchiyama M; Osada H; Takahashi S Control of the Stereochemical Course of [4+2] Cycloaddition during trans-Decalin Formation by Fsa2-Family Enzymes. Angew. Chem. Int. Ed. Engl 2018, 57, 9754–9758. [PubMed: 29972614]
24. Kakule TB; Lin Z; Schmidt EW Combinatorialization of Fungal Polyketide Synthase-Peptide Synthetase Hybrid Proteins. J. Am. Chem. Soc 2014, 136, 17882–17890. [PubMed: 25436464]
25. National Committee for Clinical Laboratory Standards. Reference Method for Broth Dilution Antifungal Susceptibility Testing of Yeasts. Approved Standard M27-A NCCLS Wayne, USA 2008.
26. Frisch MJ et al. Gaussian 09, revision D.01; Gaussian, Inc.: Wallingford, CT, 2013 (See SI for full citation)
27. Zhao Y; Truhlar DG Density Functionals with Broad Applicability in Chemistry. Acc. Chem. Res 2008, 41, 157–167. [PubMed: 18186612]
28. Cossi M; Rega N; Scalmani G; Barone V Energies, Structures and Electronic Properties of Molecules in Solution With the C-PCM Solvation Model. J. Comp. Chem 2003, 24, 669–681. [PubMed: 12666158]
29. Tang MC; Lin HC; Li DH; Zou Y; Li J; Xu W; Cacho RA; Hillenmeyer ME; Garg NK; Tang Y Discovery of Unclustered Fungal Indole Diterpene Biosynthetic Pathways through Combinatorial Pathway Reassembly in Engineered Yeast. J. Am. Chem. Soc 2015, 137, 13724–13727. [PubMed: 26469304]
30. Zaghouani M; Nay B 3-Acylated Tetramic and Tetronic Acids as Natural Metal Binders: Myth or Reality? Nat. Prod. Rep 2016, 33, 540–548. [PubMed: 26879987]

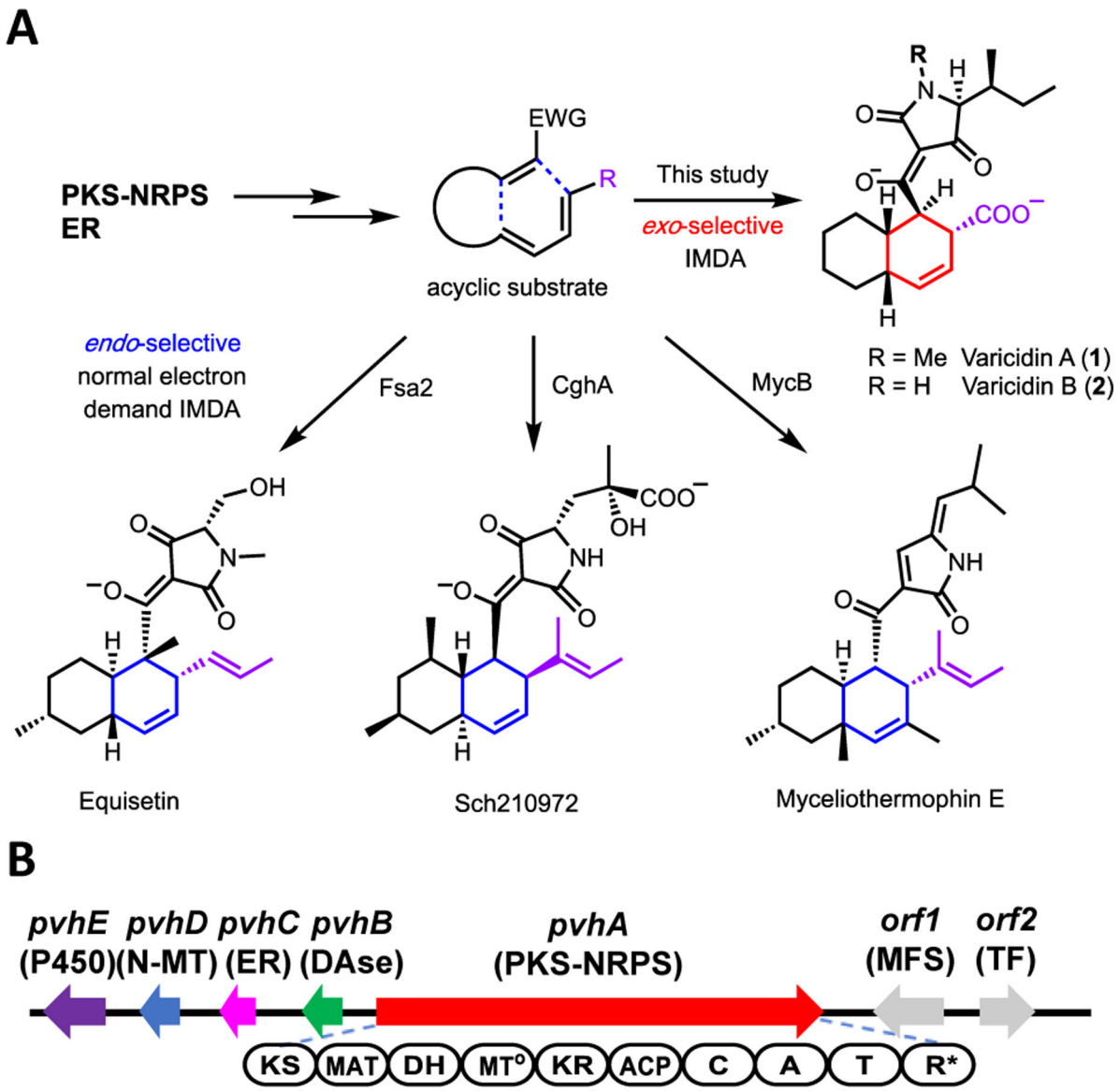


**Figure 1.**

Lipocalin-like DAses catalyzes IMDA reactions in biosynthesis of decalin-containing fungal NPs. (**A**) Characterized DAses and their decalin containing products; (**B**) Genome mining of a DAse (PvhB) containing cryptic gene cluster from *P. variable.* Abbreviations: KS, ketosynthase; MAT, malonyl-CoA transferase; DH, dehydratase; MT, methyltransferase; KR, ketoreductase; ACP, acyl carrier protein; C, condensation; A, adenylation; T, thiolation; R, reductase. MFS: major facilitator superfamily; TF: transcription factor; *N*-MT: *N*-methyltransferase; ER: enoylreductase; DAse: Diels-Alderase.

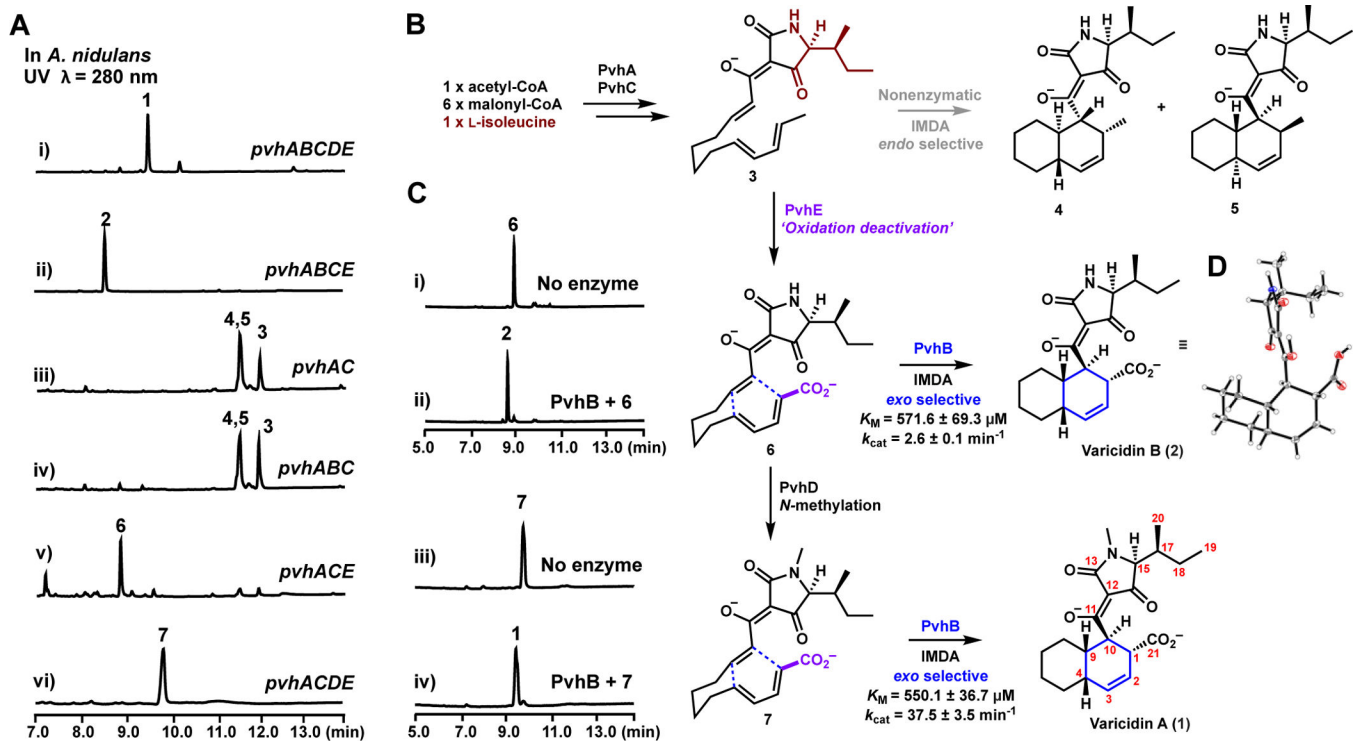


**Figure 2.**

Biosynthesis of varicidin A **1**. (**A**) Product profiles of *A. nidulans* transformed with combinations of *pvh* genes; (**B**) The proposed biosynthetic pathway of **1**; (**C**) Biochemical characterization of the DAse PvhB *in vitro*. The traces are HPLC with λ = 280 nm. (**D**) Crystal structure of **2** (see CIF file as supporting information).

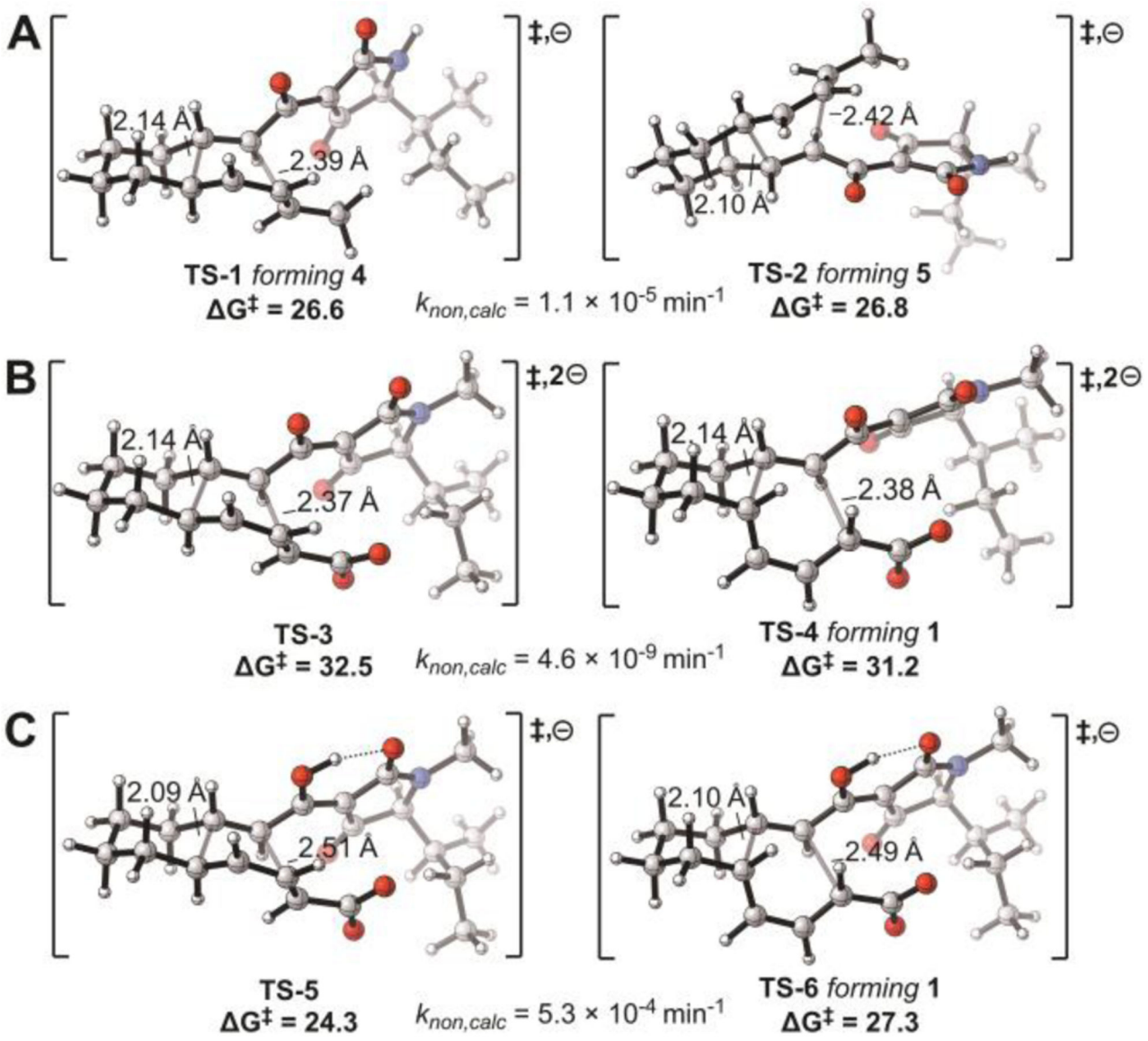


**Figure 3.**

DFT calculated transition states of NEDDA and IEDDA. (**A**) Transition state structures **TS-1** and **TS-2** with energies shown for nonenzymatic *endo*-cyclizations of **3** forming **4** and **5**, respectively. (**B**) *endo* **TS-3** and *exo* **TS-4** of IEDDA reactions in solution as dianions. **TS-4** leads to formation of the *cis*-decalin stereochemistry for varicidin A. (**C**) *endo* **TS-5** and *exo* **TS-6** of NEDDA reactions when tetramic acid is protonated.